Chlamydomonas FAP133 is a dynein intermediate chain associated with the retrograde intraflagellar transport motor

Panteleimon Rompolas[1], Lotte B. Pedersen[2], Ramila S. Patel-King[1] and Stephen M. King[1,*]

[1]Department of Molecular, Microbial and Structural Biology, University of Connecticut Health Center, Farmington, CT 06030, USA
[2]Department of Molecular Biology, University of Copenhagen, Universitetsparken 13, DK-2100 Copenhagen, Denmark
*Author for correspondence (e-mail: king@neuron.uchc.edu)

Accepted 28 August 2007
Journal of Cell Science 120, 3653-3665 Published by The Company of Biologists 2007
doi:10.1242/jcs.012773

Summary

Intraflagellar transport (IFT) is the bi-directional movement of particles along the length of axonemal outer doublet microtubules and is needed for the assembly and maintenance of eukaryotic cilia and flagella. Retrograde IFT requires cytoplasmic dynein 1b, a motor complex whose organization, structural composition and regulation is poorly understood. We have characterized the product of the *Chlamydomonas FAP133* gene that encodes a new WD-repeat protein similar to dynein intermediate chains and homologous to the uncharacterized vertebrate protein WD34. FAP133 is located at the peri-basal body region as well as in punctate structures along the flagella. This protein is associated with the IFT machinery because it is specifically depleted from the flagella of cells with defects in anterograde IFT. Fractionation of flagellar matrix proteins indicates that FAP133 associates with both the LC8 dynein light chain and the IFT dynein heavy chain and light intermediate chain (DHC1b-D1bLIC) motor complex. In the absence of DHC1b or D1bLIC, FAP133 fails to localize at the peri-basal body region but, rather, is concentrated in a region of the cytoplasm near the cell center. Furthermore, we found that FAP133, LC8, DHC1b, D1bLIC, the FLA10 kinesin-2 necessary for anterograde IFT and other IFT scaffold components associate to form a large macromolecular assembly.

Key words: *Chlamydomonas*, Cilia, Dynein, Flagella, Intraflagellar transport

Introduction

In eukaryotic cilia and flagella, intraflagellar transport (IFT) is the bi-directional movement of large protein complexes along the length of axonemal outer doublet microtubules (Rosenbaum and Witman, 2002; Scholey, 2003). IFT was first observed in *Chlamydomonas reinhardtii* (Kozminski et al., 1993), and it was later shown that IFT is a highly conserved process, necessary for assembling and maintaining cilia in evolutionary distant organisms such as *Caenorhabditis elegans* and humans (Cole et al., 1998; Rosenbaum and Witman, 2002). Cilia and flagella are assembled and continuously turnover at their distal tip (Johnson and Rosenbaum, 1992; Marshall and Rosenbaum, 2001; Witman, 1975), and it is thought that IFT mediates the transport of flagellar components from the basal body region to their assembly site as well as the removal of turnover products from the flagellar tip (Qin et al., 2004). Additionally, specific receptors and other membrane components that preferentially localize to the cilium may be transported there by IFT (Christensen et al., 2007; Pan et al., 2005).

IFT particles have been isolated from *Chlamydomonas* flagella and found to consist of two biochemically distinct complexes, A and B, which collectively comprise at least 17 different IFT particle proteins (Cole et al., 1998; Piperno and Mead, 1997; Cole, 2003). Most complex A and complex B proteins are highly conserved among different organisms, and mutant analyses in *Chlamydomonas* and *C. elegans* have shown that many IFT proteins are essential for flagellar and ciliary assembly (Cole, 2003), although specific functions have been ascribed to only a few. For example, IFT172 interacts with the microtubule plus-end-binding protein EB1 and is believed to regulate the anterograde-retrograde IFT transition at the flagellar tip (Pedersen et al., 2005). Additionally, IFT20 may regulate the transport of membrane bound proteins from the Golgi complex to the cilium (Follit et al., 2006), and another complex B protein, IFT27, was recently shown to be involved in cell cycle control (Qin et al., 2007). Moreover, analysis of a partial suppressor mutation in *IFT46* suggests that the IFT46 protein is required for transporting outer dynein arms (Hou et al., 2007).

IFT particles together with cargo proteins are ferried to the ciliary tip by a plus-end-directed heterotrimeric kinesin-2 that has been well characterized in several model systems (Cole et al., 1993; Cole et al., 1998; Pan et al., 2006; Yamazaki et al., 1995); in some organisms, such as *C. elegans*, an additional homodimeric kinesin-2 motor OSM-3 cooperates with heterotrimeric kinesin-2 during anterograde IFT (Snow et al., 2004). The molecular motor required for retrograde IFT is cytoplasmic dynein 1b (also termed cytoplasmic dynein 2) about which comparatively little is known (Pazour et al., 1999; Porter et al., 1999; Signor et al., 1999).

Dyneins drive microtubule minus-end-directed motion in cells and are multi-protein complexes that consist of one or more heavy chains (HCs) belonging to the AAA$^+$ family of

ATPases and a number of accessory proteins required for structural integrity, regulation of motor activity and cargo specificity (reviewed in King, 2002). The major isoform of cytoplasmic dynein (cytoplasmic dynein 1 or 1a) is involved in a wide range of intracellular activities including vesicular transport, chromosome segregation and organization of the cytoplasmic microtubule network (Vallee et al., 2004). This dynein is a HC homodimer and contains two intermediate chains (ICs), two light intermediate chains (LICs) as well as at least three different light chain (LC) dimers of the LC8 (DYNLL), Roadblock/LC7 (DYNLRB) and Tctex1 (DYNLT) families (Pfister et al., 2006). By contrast, to date only three proteins – an isoform-specific HC (DHC1b) and LIC (D1bLIC), and possibly LC8 – have been identified as components of the cytoplasmic dynein that drives retrograde IFT. In *Chlamydomonas*, null mutations of *DHC1b* result in impaired ability to grow flagella of normal length. Instead, these cells assemble stumpy flagella with large accumulations of IFT particles at their tip, suggesting a defect in retrograde IFT (Pazour et al., 1999). In *C. elegans*, this dynein is required for retrograde transport in chemosensory cilia (Signor et al., 1999), and the mammalian ortholog is enriched in ciliated epithelia and localizes at the connecting cilia in the retinal epithelium and in primary cilia of cultured cells (Mikami et al., 2002), indicating a conserved function in ciliary assembly.

A LIC (D1bLIC) was identified first in mammals and subsequently in *Chlamydomonas* and *C. elegans*, as an integral component of the retrograde IFT dynein complex (Grissom et al., 2002; Hou et al., 2004; Perrone et al., 2003; Schafer et al., 2003). In *Chlamydomonas* a null mutation in *D1bLIC* also results in stumpy flagella with large accumulations of IFT particles (Hou et al., 2004). Moreover, LC8 – which is a highly conserved component of both cytoplasmic and axonemal dyneins as well as other enzyme complexes – is also thought to play a role in retrograde IFT, because the *Chlamydomonas* LC8-null mutant strain (*fla14*) exhibits defects in this process (Pazour et al., 1998). However, to date there is no direct evidence that LC8 is part of the same complex as DHC1b and D1bLIC.

Although cytoplasmic and axonemal dyneins containing more than one HC associate with two ICs that belong to the WD-repeat protein family, no such IC has yet been identified for the retrograde IFT motor. In an effort to fully understand the dynein motor complex that powers retrograde IFT, we have characterized the product of the *Chlamydomonas* gene *FAP133*, which encodes a protein similar to other dynein ICs and has conserved homologs in vertebrates and many other ciliated organisms. We show, using genetic, biochemical and immunofluorescence approaches, that FAP133 is part of the IFT machinery in *Chlamydomonas*. Furthermore, we provide biochemical evidence that FAP133 associates specifically with DHC1b-D1bLIC and that LC8 is also part of this complex. Together, these results suggest that FAP133 is a component of the retrograde dynein motor and plays a conserved role in retrograde IFT.

Results

Molecular characterization of *Chlamydomonas FAP133*

As many dyneins associate with WD-repeat intermediate chains (ICs), to identify a putative IC associated with the IFT dynein motor complex we searched the *Chlamydomonas* genomic and EST databases using the protein sequence of the rat cytoplasmic dynein IC (DYNC1I2; accession Q62871) as a query. We identified a previously uncharacterized gene consisting of 12 exons that has subsequently been annotated as *FAP133* (JGI version 2.0, scaffold 2:870454-873524) and obtained a full-length cDNA clone (BP095745) from the Kazusa DNA Research Institute, Chiba, Japan. Southern blot analysis of *Chlamydomonas* genomic DNA using the *FAP133* cDNA as a probe, confirmed that there is a single gene for FAP133 (Fig. 1A). Moreover, expression of *FAP133* results in a ~2.5 kb message that is upregulated upon deflagellation (Fig. 1B), which is a common property of mRNAs that encode flagellar proteins (Stolc et al., 2005).

The *FAP133* cDNA is predicted to encode a 558-residue protein with a mass of 61,160 Da and pI of 5.34. Database searches and sequence alignment revealed that FAP133 is most closely related to the uncharacterized vertebrate protein WD34 [$P_{(n)}=2\times e^{-68}$ vs the zebrafish (*Danio*) homolog; accession BC133909; Fig. 1C]. Furthermore, domain analysis identified six WD-repeat domains within the C-terminal region of FAP133 (Fig. 1D), similar to other dynein ICs (Ogawa et al., 1995; Wilkerson et al., 1995); the region between the third and fourth domains (residues 295-392) may contain a seventh degenerate WD-repeat. FAP133 also contains two putative degenerate LC8 binding sites (Lo et al., 2001) near the N-terminus, VETQT (residues 46-50) and QGTQT (residues 56-60) (Fig. 1D).

FAP133 is located in flagella and at the peri-basal body region

In the recently published *Chlamydomonas* flagellar proteome (Pazour et al., 2005), FAP133 peptides were primarily found in the detergent-soluble flagellar membrane and matrix fraction, similar to DHC1b and other IFT proteins. To further characterize the molecular properties of FAP133, we raised a specific antiserum (CT248) against a recombinant FAP133 peptide (residues 89-558), expressed as a C-terminal fusion with maltose-binding protein. Immunoblot analysis of isolated wild-type *Chlamydomonas* flagella revealed that the affinity-purified CT248 antibody specifically recognized a single band migrating at M_r ~66,000 (Fig. 2A). To identify the specific flagellar compartment(s) in which FAP133 is located, we extracted flagellar matrix proteins by subjecting isolated flagella to repeated freeze-thaw cycles in order to mechanically disrupt the membrane, or treated flagella with a non-ionic detergent to solubilize both membrane and matrix proteins. In both cases the majority of FAP133 was found in the soluble fraction with lesser amounts remaining associated with the axoneme (Fig. 2B,C). We next tested whether ATP would induce the release of the FAP133 fraction that remained associated with the axoneme after detergent extraction, as is the case with the heterotrimeric kinesin-2 and DHC1b polypeptides (Henson et al., 1997; Pazour et al., 1999). ATP treatment, indeed, caused a portion of FAP133 to detach from the axonemes; a similar amount of D1bLIC was also released. However, subsequent ATP additions did not solubilize more protein. The remaining axoneme-bound FAP133 was extracted with 0.6 M NaCl as was an additional fraction of D1bLIC and most of the outer arm dynein component LC2 (Fig. 2C).

To further define the flagellar location of FAP133 in wild-type *Chlamydomonas* cells, we performed immuno-

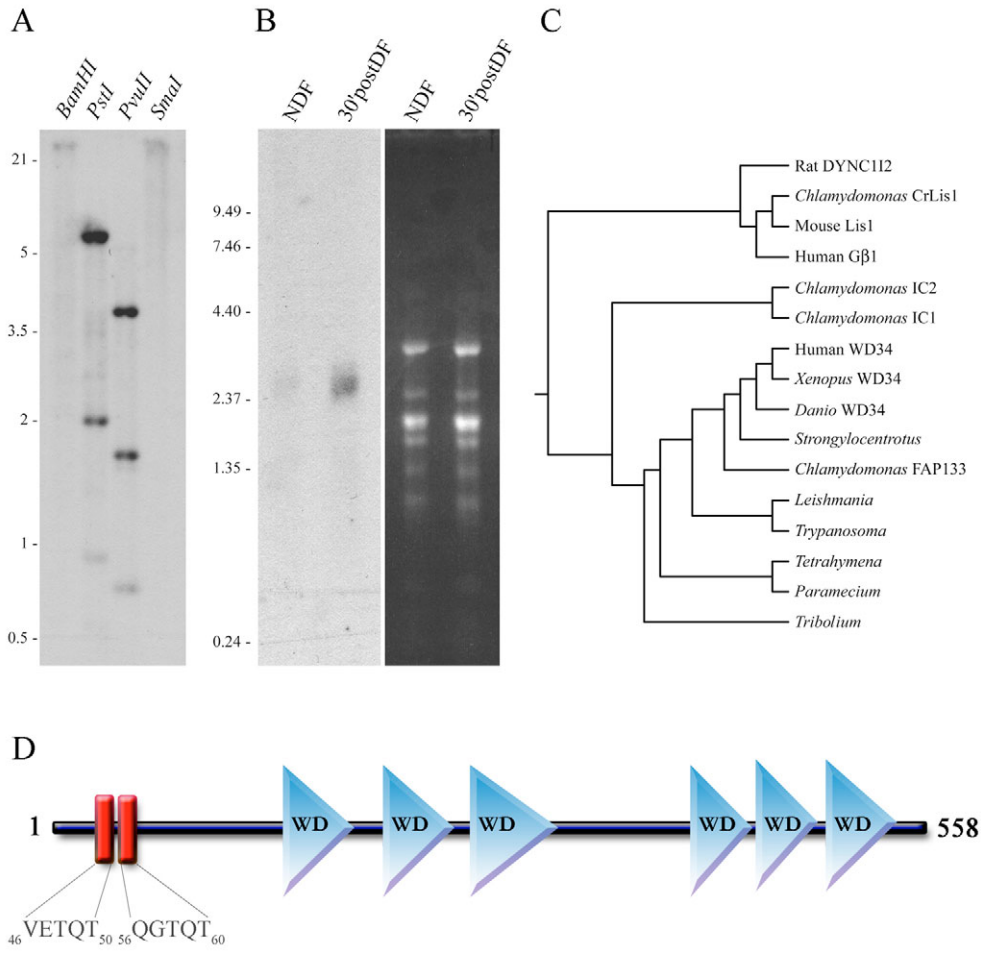

Fig. 1. Molecular characterization of *Chlamydomonas* FAP133. (A) Southern blot analysis of restricted *Chlamydomonas* genomic DNA, using the FAP133 cDNA as a probe. The blot reveals single bands in *Bam*HI- and *Sma*I-digested samples indicating that there is a single *FAP133* gene present in the *Chlamydomonas* genome. (B) Northern blot analysis of *Chlamydomonas* RNA demonstrating upregulation by ~460% of the ~2.4 kb *FAP133* transcript 30 minutes after deflagellation (30′postDF) compared to non-deflagellated cells (NDF). The right panel shows the ethidium-bromide-stained gel used for the analysis; quantitation of the upper three bands revealed that the amount in the NDF sample was 78%, 99% and 72% that of the 30′postDF sample, respectively. (C) Neighbor-joining tree showing the relationship of *Chlamydomonas* FAP133 to other proteins containing WD-repeats. Phylogenetic analysis was based on a CLUSTALW alignment of FAP133 with *Chlamydomonas* outer-arm IC1 (Q39578) and IC2 (P27766), *Chlamydomonas* CrLis1 (ABG33844), mouse Lis1 (P63005), human Gβ1 (P62873), rat cytoplasmic dynein DYNC1I2 (Q62871), human, *Xenopus* and *Danio* WD34 proteins (NM_052844, BC106359 and BC133909, respectively), and uncharacterized proteins from *Strongylocentrotus purpuratus* (XM_001197794), *Leishmania infantum* (XM_001466479), *Trypanosoma brucei* (XP_839051), *Tetrahymena thermophila* (XM_001022425), *Paramecium tetraurelia* (XM_001458772) and *Tribolium castaneum* (XM_966966). FAP133 is most closely related to the vertebrate WD34 proteins. (D) Sequence analysis of the *Chlamydomonas* FAP133 protein, using the SMART algorithm, revealed six WD-repeat domains that probably form a β-propeller. Two degenerate putative LC8-binding sites, VETQT (residues 46-50) and QGTQT (residues 56-60), are located in the N-terminal part of the molecule.

fluorescence microscopy with the CT248 antibody. The analysis revealed that the great majority of FAP133 localized to a bi-lobed area near the basal bodies (Fig. 2D). In addition, FAP133 was found in numerous puncta that were randomly distributed along the entire length of both flagella. This localization is remarkably similar to that observed previously for IFT particle subunits and motors (e.g. Hou et al., 2004; Pazour et al., 1999).

FAP133 requires FLA10 kinesin-2 for flagellar localization

To further investigate the possible association of FAP133 with the IFT machinery, we employed a *Chlamydomonas* strain with a temperature-sensitive mutation in the *FLA10* gene, which encodes the 90 kDa motor unit of the heterotrimeric kinesin-2 that powers anterograde IFT (Huang et al., 1977; Kozminski et al., 1995; Walther et al., 1994). If grown at 22°C, *fla10* cells can form flagella of normal length that are virtually indistinguishable from wild-type flagella. When the temperature is raised to 32°C, *fla10* flagella become depleted of IFT particle proteins within the first 1-2 hours as a result of stalled anterograde IFT but still active retrograde IFT (Cole et al., 1998); DHC1b and D1bLIC also become depleted from *fla10* flagella under these conditions (Iomini et al., 2001; Pedersen et al., 2006). We found that the protein levels of FAP133 in *fla10* flagella were dramatically reduced after only 1 hour at the restrictive temperature, in contrast to other axonemal proteins, such as IC1, which was

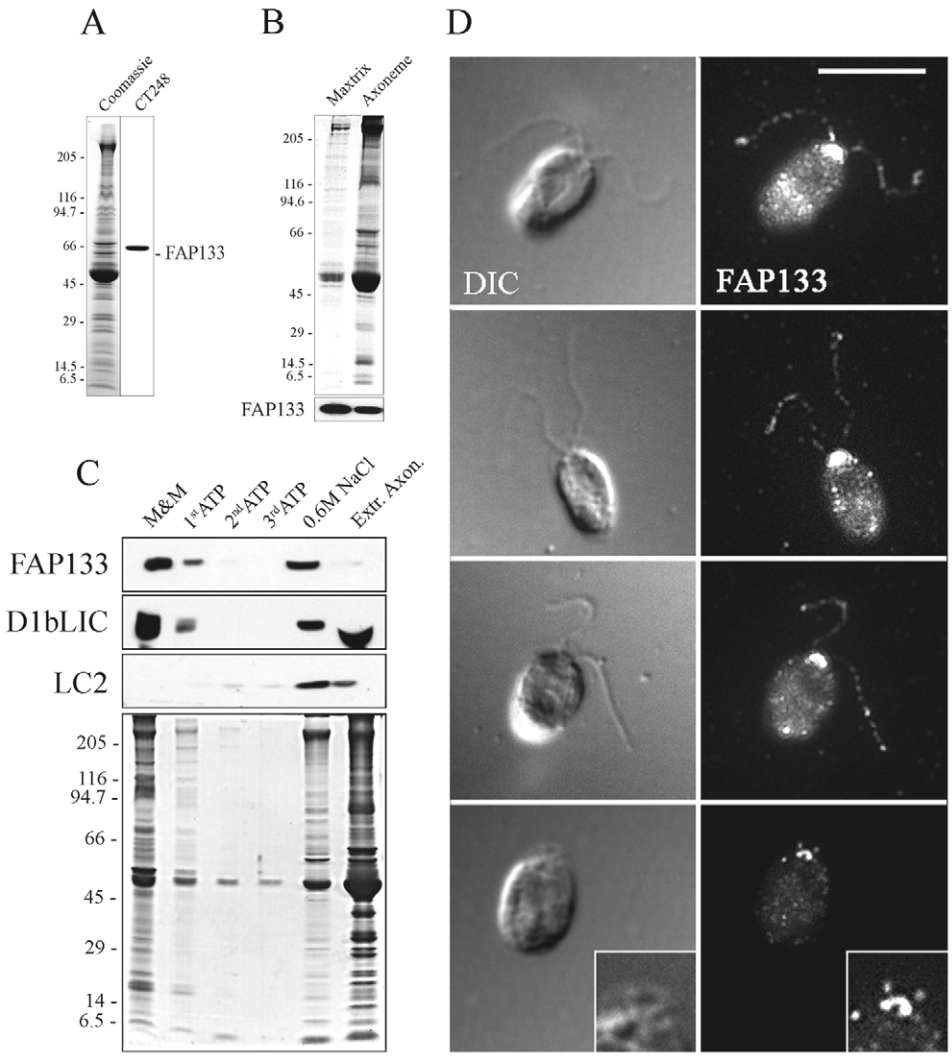

Fig. 2. Localization of FAP133 to flagella and the peri-basal body region. (A) Purified *Chlamydomonas* flagella were separated in a 5-15% polyacrylamide gel and stained with Coomassie Blue (left) or blotted to nitrocellulose membrane for immunodetection (right). Rabbit polyclonal antibody (CT248) raised against FAP133 specifically recognized a single band of M_r~66,000. (B) Equivalent amounts of flagella matrix proteins obtained by freeze-thaw and extracted flagella were separated in a 5-15% polyacrylamide gel and stained with Coomassie Blue (upper panel) or transferred to nitrocellulose and probed with CT248 to detect FAP133 (lower panel). The majority of FAP133 was found in the flagellar matrix fraction. (C) Membrane and matrix proteins were initially extracted from isolated flagella with detergent (M&M). The resulting axonemes were incubated three times with a buffer that contained 10 mM ATP (1st, 2nd and 3rd ATP respectively). Finally ATP-treated axonemes were extracted with a high-salt buffer (0.6 M NaCl). Equivalent amounts of these fractions and the axonemal remnants (Extr. Axon.), were separated in a 5-15% polyacrylamide gel and stained with Coomassie Blue (lower panel) or transferred to nitrocellulose membrane and probed with antibodies against FAP133, D1bLIC and LC2 (upper panels). (D) *Chlamydomonas* cells were prepared for indirect immunofluorescence microscopy using the CT248 antibody against FAP133. Images were acquired using differential interference contrast optics (left panels) to show the location of the two flagella and also under fluorescence (right panels) to detect the FAP133-specific signal. FAP133 localized primarily to the peri-basal body region as well as in punctate structures along the flagella. Images of the cell in the bottom panel were acquired while focusing at the basal body region and insets show enlargements of this area. Bar, 10 μm.

not affected by the temperature shift (Fig. 3A). This finding was confirmed by immunofluorescence microscopy, which also revealed that almost all FAP133 protein in *fla10* cells incubated at 32°C was located at the peri-basal body region; by contrast, FAP133 was readily detected in the flagella of wild-type cells at this temperature (Fig. 3B). These results indicate that FAP133 depends on FLA10 kinesin-2 for flagellar localization as do IFT particle proteins and IFT dynein motor subunits suggesting that FAP133 associates specifically with IFT. To further test this, we compared FAP133 incorporation into wild-type flagella and mutants lacking outer arms alone (*oda6*), outer arms and the docking complex (*oda3*), outer arms and the Oda5p/adenylate kinase complex (*oda5*), inner arm I1/f (*ida1*), inner arms a, c and d (*ida4*), radial spokes (*pf14*) and the central pair microtubule complex (*pf18*). Immunoblot analysis revealed that FAP133 was present at essentially wild-type levels in all mutant strains (Fig. 4).

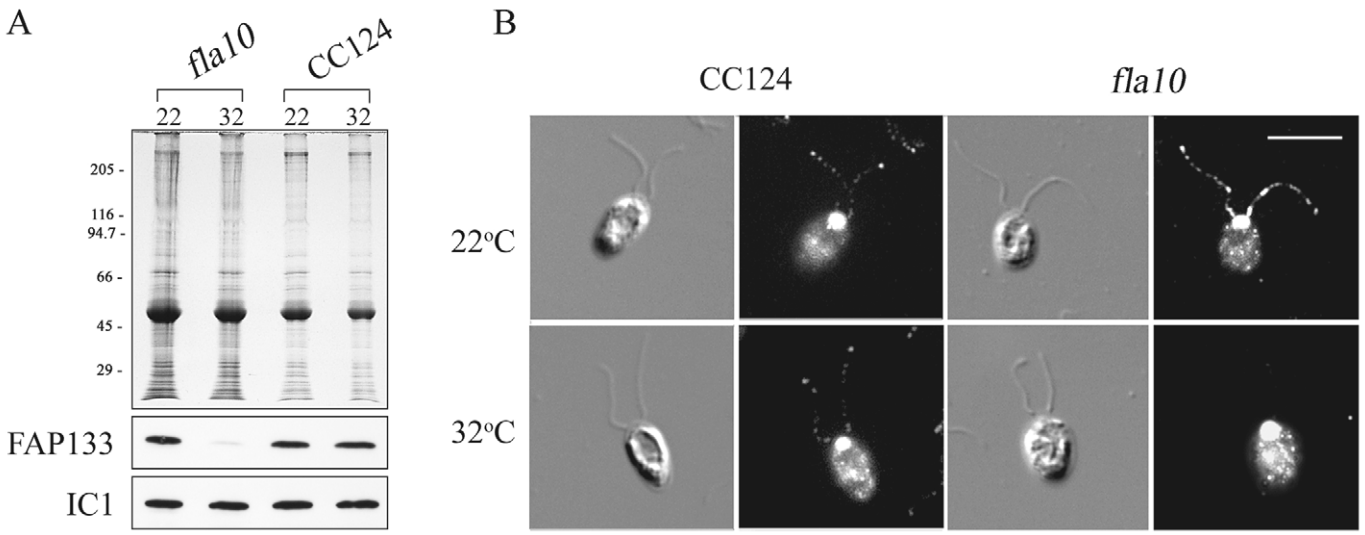

Fig. 3. Flagellar localization of FAP133 requires anterograde IFT. (A) Flagella were isolated from wild-type (CC124) and *fla10* cells (harbors a temperature-sensitive mutation in the *FLA10* kinesin-2 gene) after incubation for 1 hour at either the permissive temperature of 22°C or the restrictive temperature of 32°C. Flagellar proteins were separated in a 5-15% polyacrylamide gel and either stained with Coomassie Blue (upper panel) or transferred to nitrocellulose and probed with antibodies against FAP133 and outer dynein arm protein IC1 (lower panels). FAP133 levels are reduced in the *fla10* strain only at the restrictive temperature. (B) Wild-type and *fla10* cells, under the same conditions as in (A), were fixed and processed for indirect immunofluorescence microscopy using the FAP133 antibody. The punctate FAP133 signal was absent only from the flagella of *fla10* cells at the restrictive temperature.

FAP133 co-fractionates with the retrograde IFT dynein

The flagellar localization pattern and *fla10* analysis described above strongly suggest that FAP133 is associated with the IFT machinery. To elucidate the specific IFT complex proteins with which FAP133 associates, we examined the hydrodynamic properties of FAP133 and other IFT components from the flagella matrix. Specifically, freshly prepared freeze-thaw flagella extracts were fractionated by sucrose-density-gradient centrifugation using a buffer of relatively low ionic strength (25 mM KCl). Under these conditions, and in agreement with previous reports (Cole et al., 1998), based on immunoblots and analysis of Coomassie-Blue-stained gels, we found IFT complex A and complex B polypeptides sedimenting at ~16 S and the heterotrimeric kinesin-2 motor (FLA10) at ~10 S (Fig. 5A). We also found that the DHC1b-D1bLIC complex sedimented in two distinct peaks; the majority of this dynein complex was at ~18 S with a smaller amount at ~12 S. Interestingly, FAP133 was also detected in two distinct peaks: a minor peak occurring at ~18 S that followed the sedimentation profile of DHC1b and D1bLIC in that region, as well as a major FAP133 peak at ~10 S. LC8 co-purified with both pools of FAP133, suggesting that these two proteins interact (and see below). These results suggest either that there are two distinct pools of FAP133 in the flagellum, or that FAP133 binds weakly to the DHC1b-D1bLIC complex and is readily dissociated from this motor complex under our experimental conditions. To distinguish between these two possibilities, we pooled the fractions corresponding to the ~18 S peak and fractionated them again in a second gradient. Again, DHC1b was present at ~18 S but FAP133 was not and instead was found only at ~10 S (Fig. 5B), suggesting that the FAP133 pool at ~10 S results from dissociation of the ~18 S complex. Interestingly, we also found that conditions which altered the sedimentation behavior of DHC1b also changed that of FAP133. Specifically, the use of 1% Tergitol to extract flagellar membrane and matrix proteins caused DHC1b to sediment as a single peak at ~12 S. Under these conditions, all FAP133 was present in a single peak at ~10 S (Fig. 5C).

FAP133–retrograde-IFT-dynein co-purifies with kinesin-2 and IFT complex A

As FAP133 readily dissociated from the ~18 S IFT dynein complex in sucrose gradients (Fig. 5A,B), possibly as a result of high hydrostatic pressure, we sought a more gentle fractionation method. For this, we extracted flagella matrix components by freeze-thaw in the absence of a detergent using a relatively low-ionic-strength extraction buffer. To separate the different complexes, we employed a Superose-6 gel-filtration column, which has an exclusion limit of ~40 MDa, equilibrated with the same low-ionic-strength buffer that was used previously for the extraction of flagella matrix proteins. Essentially all DHC1b and D1bLIC were eluted as a single peak very early from the column (fractions 2 and 3; Fig. 6A). At least 50% of total FAP133 and the FLA10 kinesin-2 subunit were also detected in these same fractions. Furthermore, the elution profile of LC8 showed three distinct peaks, of which the first two coincided with those of FAP133. Similarly, we detected two distinct peaks of the complex A protein IFT139; ~10% co-eluted with DHC1b, FAP133 and FLA10. By contrast, we obtained only a single peak of the complex B protein IFT81 that did not co-fractionate with IFT139, DHC1b or FAP133. These results confirm that FAP133 is associated with the retrograde IFT dynein complex (DHC1b, D1bLIC, LC8), and also suggest that this complex is associated with IFT complex A and kinesin-2. A similar elution profile was obtained for a flagellar extract from the mutant *pf28pf30ssh1* that lacks both outer arms and inner arm I1/f (not shown).

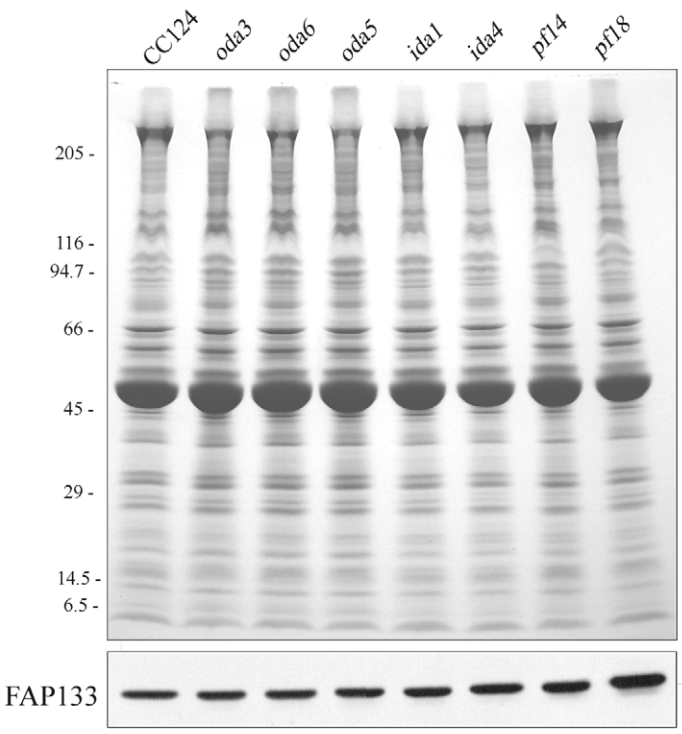

Fig. 4. FAP133 is present in strains lacking axonemal substructures. Flagella from wild-type *Chlamydomonas* (CC124) and strains lacking various axonemal substructures including the outer dynein arm alone (*oda6*) or in combination with the docking complex (*oda3*) or Oda5p-adenylate kinase complex (*oda5*), inner dynein arm I1/f (*ida1*), inner arms a, c and d (*ida4*), the radial spokes (*pf14*) and central pair microtubule complex (*pf18*) were electrophoresed in a 5-15% polyacrylamide gradient gel and stained with Coomassie Blue (upper panel) or blotted and probed with antibody against FAP133 (lower panel). All mutant strains contain essentially wild-type levels of FAP133.

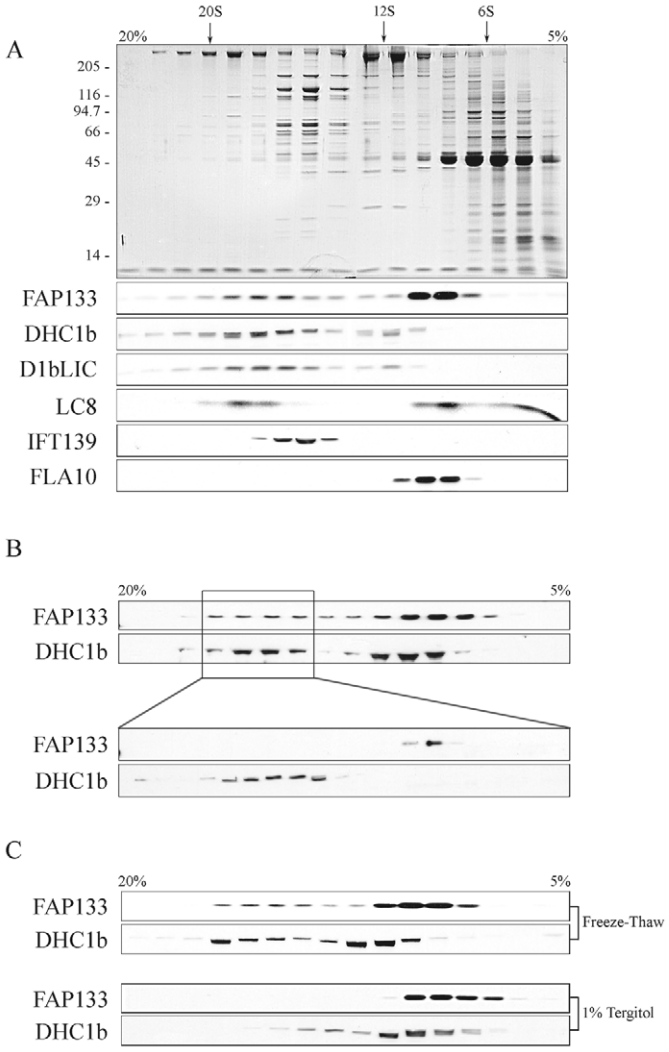

Fig. 5. FAP133 co-purifies with DHC1b-D1bLIC in sucrose density gradients. (A) Flagellar matrix proteins were separated in a 5 ml 5-20% sucrose density gradient and the resulting fractions were analyzed in two 5-15% polyacrylamide gels and stained with Coomassie Blue (upper panel); similar gels were blotted onto nitrocellulose membrane for immunodetection (lower panels), using antibodies against FAP133, DHC1b, D1bLIC, LC8, IFT139 and FLA10. (B) Fractions 4-7 from a similar gradient (upper panel) were pooled, the sucrose removed and the concentrated sample layered on a separate 5 ml 5-20% sucrose density gradient (lower panel). Immunoblots from both gradients were probed for FAP133 and DHC1b. FAP133 that originally sedimented at ~18 S during the first fractionation shifted to ~10 S in the second gradient suggesting that the FAP133-containing complex had dissociated. (C) Flagellar matrix proteins (Freeze-Thaw; upper panels) or detergent-soluble flagellar membrane and matrix extract (1% Tergitol; lower panels) were fractionated in two separate sucrose-density gradients and analyzed for FAP133 and DHC1b. Detergent treatment caused all DHC1b and FAP133 to migrate more slowly than when obtained by freeze-thaw.

To further test whether these proteins are part of the same complex we immunoprecipitated FAP133 and IFT139 from freshly prepared flagella-matrix extracts, using CT248 and a monoclonal IFT139-specific antibody (Cole et al., 1998), respectively. Both pellets contained FAP133, DHC1b-D1bLIC, IFT139 and FLA10 polypeptides: control proteins (IC1 and EB1) were not detected in the precipitates; D1bLIC co-migrates with the FAP133 polyclonal antibody heavy chain band and, thus, any potential signal in that precipitate was obscured (Fig. 6B,C). Moreover, in the FAP133 pellet we detected a considerable amount of LC8, suggesting a strong interaction between these two proteins (see below) and also some IFT81 (Fig. 6B). When we immunoprecipitated IFT172 from complex B, we found IFT81 and a very small amount of IFT139 but no dynein or kinesin components in the pellet (Fig. 6D). These data are somewhat different to those reported by (Pedersen et al., 2006) and probably stem from differences in extract preparation or other experimental conditions.

FAP133 requires DHC1b and D1bLIC for localization at the peri-basal body region

Previous work has shown that the level of D1bLIC is dramatically reduced in *dhc1b*-null mutant cells and that DHC1b levels are reduced in the *d1blic*-null strain (Hou et al., 2004). Moreover, DHC1b is required for localization of D1bLIC at the basal bodies, but D1bLIC is not required for

basal-body localization of DHC1b (Hou et al., 2004; Perrone et al., 2003). To determine whether the protein levels and subcellular localization of FAP133 are affected by the absence of specific subunits of the retrograde IFT dynein motor, we employed three *Chlamydomonas* null mutant strains; *dhc1b*, *d1blic* and *fla14*, which lack the *DHC1b*, *D1bLIC* and *LC8* genes, respectively (Hou et al., 2004; Pazour et al., 1999; Pazour et al., 1998). All three of these mutants are defective in retrograde IFT and have small and stumpy flagella that accumulate IFT particle components. We prepared whole-cell extracts from these mutant strains and analyzed them by immunoblotting. FAP133 levels were similar in wild-type and in the *dhc1b* and *d1blic* mutant cells, but showed a modest decrease in *fla14* (Fig. 7A). By contrast, DHC1b was essentially undetectable in both *d1blic* and *fla14* strains, whereas levels of D1bLIC were reduced in both *dhc1b* and *fla14*. Finally, the amount of LC8 present in wild-type as well as *dhc1b* and *d1blic* mutant cells did not vary significantly (Fig. 7A), consistent with the participation of this protein in many functionally distinct complexes.

We next used immunofluorescence microscopy to examine the subcellular localization of FAP133 in these mutant strains. We detected a striking difference in the distribution of FAP133 between wild-type and the *dhc1b* or *d1blic* mutant cells. Specifically, in the absence of DHC1b or D1bLIC, FAP133 was almost completely redistributed from the peri-basal body region, was present throughout the cytoplasm and most prominently occurred in a zone near the cell center where the Golgi usually resides (Fig. 7B). By contrast, the absence of LC8 did not alter the normal localization of FAP133 at the basal bodies, but we could not detect this protein in the *fla14* flagella stubs. The redistribution of FAP133 in the *dhc1b* and *d1blic* mutants was specific because in all strains used here, the FLA10 kinesin-2 subunit, and complex A and complex B proteins were located either at the basal bodies, or accumulated in the flagella stubs (data not shown). In summary, these results suggest that DHC1b and D1bLIC are required for targeting and/or tethering of FAP133 near the basal bodies, potentially as a result of incorporation into the dynein holoenzyme, but they do not affect the stability of this protein in cytoplasm. By contrast, LC8 is not required for localizing FAP133 to the basal bodies but might affect the stability of FAP133 and its transport into the flagella.

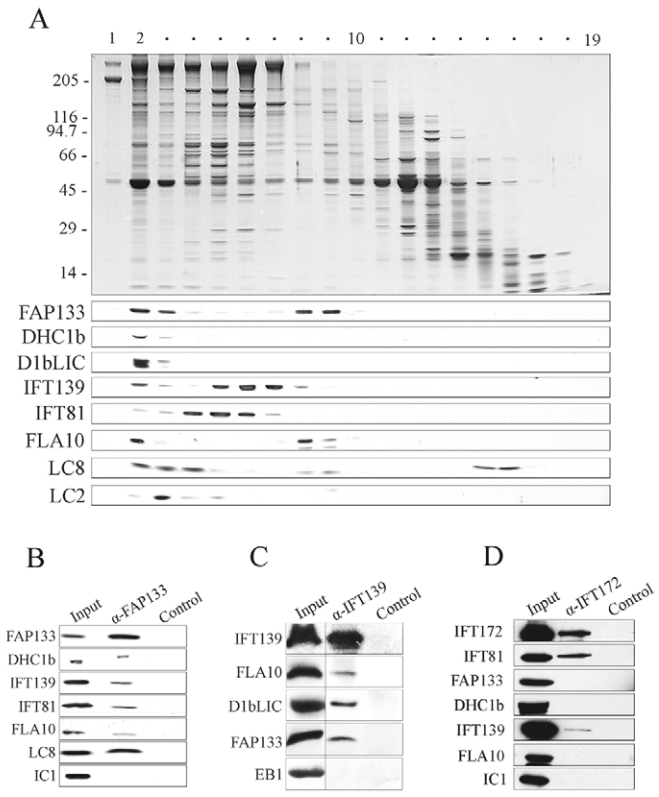

Fig. 6. FAP133 associates with other IFT proteins in a large macromolecular complex. (A) Flagella matrix components were fractionated using a Superose-6 gel filtration column. The eluted fractions were separated in two 5-15% polyacrylamide gels and stained with Coomassie Blue (upper panel); similar gels were transferred to nitrocellulose and probed with the indicated antibodies (lower panels). A significant amount of FAP133 was found in fraction 2, co-purifying with DHC1b-D1bLIC as well as clear peaks of LC8, FLA10 and the complex A protein IFT139. This fraction contained particles of >~2 MDa as outer arm dynein components (e.g. LC2) eluted in later fractions. Note that the LC8 peak is more spread out towards later fractions as this protein is also an integral component of the outer dynein arm and of inner arm I1/f. (B) Protein G-agarose beads which were previously treated with antibody against FAP133 (α-FAP133) or BSA alone (control), were incubated with flagella matrix extracts, and proteins present in the pellet and extract (10% input) were identified by immunoblotting using the indicated antibodies against various IFT proteins. An antibody against IC1 which is an outer-dynein-arm component (see DiBella and King, 2001) was included as a negative control. (C) In a similar experiment, flagellar matrix extracts were incubated with an antibody against IFT139 (α-IFT139) or an equivalent volume of PBS (control) followed by incubation with protein-G–agarose beads. The immunoprecipitated pellets were analyzed for the presence of IFT proteins by immunoblotting. The antibody against EB1 [a plus-end microtubule binding protein that localizes to the flagellar tip and basal bodies (Pedersen et al., 2003)] was used as a negative control. (D) The complex B protein IFT172 was immunoprecipitated from a flagellar extract using the anti-IFT172 antibody (α-IFT172); the control sample contained BSA alone. Only another complex B protein (IFT81) and a small amount of IFT139 from complex A were found in the pellet; DHC1b, FAP133, FLA10 and outer arm IC1 were not detected.

FAP133 associates with LC8

LC8 has been assumed to be part of the retrograde IFT motor complex because the absence of LC8 in *Chlamydomonas* results in defects in this process (Pazour et al., 1998); however, it was not observed to copurify with the DHC1b-D1bLIC complex (Perrone et al., 2003). We found that LC8 co-purified with FAP133 in sucrose gradients (Fig. 5A) and following gel filtration (Fig. 6A). In addition, LC8 was particularly enriched in the pellet of flagella-matrix proteins that were immunoprecipitated with an antibody against FAP133 (Fig. 6B). To further examine the possible interaction of LC8 with FAP133, we fractionated flagella matrix extracts using anion-exchange chromatography. Immunoblot analysis of the eluted fractions revealed two distinct peaks of FAP133 (Fig. 8). We separately pooled the fractions that contained these two peaks and layered them over two sucrose density gradients to further purify the complexes that contained FAP133. We found that FAP133 and LC8 co-sedimented at ~10 S in both gradients (Fig. 8), strongly suggesting that these proteins are part of the same complexes.

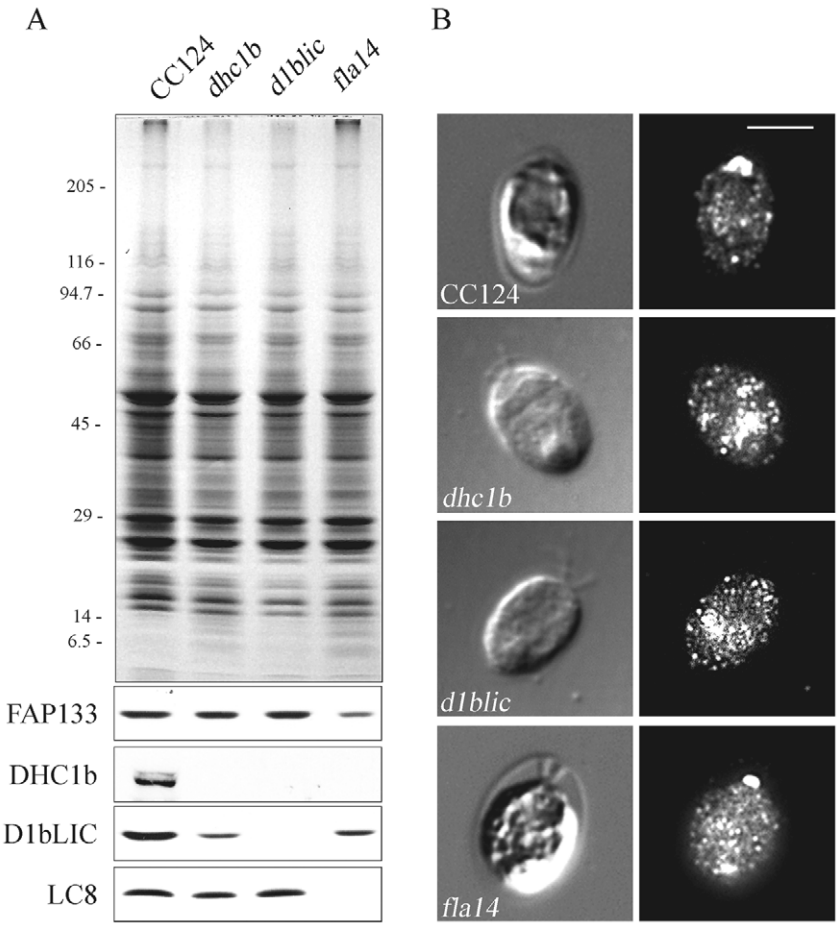

Fig. 7. FAP133 Requires DHC1b and D1bLIC for localization to the peri-basal body region. (A) Whole-cell extracts from wild-type (CC124), *dhc1b*, *d1blic* and *fla14* cells, were either stained with Coomassie Blue (upper panel) or analyzed by immunoblotting, using antibodies against FAP133, DHC1b, D1bLIC and LC8 (lower panels). (B) Indirect immunofluorescence microscopy of wild-type (CC124), *dhc1b*, *d1blic* and *fla14* cells using the antibody against FAP133. FAP133 is located primarily at the peri-basal body region in wild-type and *fla14* cells but not in the *dhc1b* or *d1blic* mutants where it is found in the cytoplasm, concentrated near the middle of the cell. Bar, 5 μm.

Discussion

In this study, we have characterized the *Chlamydomonas FAP133* gene and have shown that it encodes a novel IC that associates with the retrograde IFT dynein motor. We have also provided evidence that FAP133 interacts strongly with LC8, suggesting that this LC is also an integral component of this motor complex. Furthermore, we have found that conditions that help stabilize the interaction between FAP133/LC8 and DHC1b-D1bLIC also permit other IFT proteins, such as the FLA10 kinesin-2 subunit and IFT139, to associate with the same complex, thus providing insight into the mechanism(s) by which IFT motors assemble with the IFT particle scaffold.

FAP133 is a component of the IFT system

FAP133 is encoded by a single gene in *Chlamydomonas* that is upregulated upon deflagellation, similar to other genes that code for flagellar proteins (Stolc et al., 2005). Our findings that FAP133 is located primarily at the peri-basal body region of the cell and in punctate structures along the flagella, and that it is readily extracted from the flagella when the membrane is disrupted, suggested a role for FAP133 in IFT. This hypothesis was further supported by our observation that FAP133 is specifically depleted, together with other IFT components, from the flagella of *fla10* cells (temperature-sensitive mutant for the anterograde IFT FLA10 kinesin-2 subunit), shortly after being transferred to the restrictive temperature. In addition, we found that FAP133 protein levels were similar to wild type in the flagella of various *Chlamydomonas* mutant strains that lack specific axonemal components, including the outer arm and inner arm dynein complexes, the radial spokes or the central pair microtubules. Taken together, these observations indicate that FAP133 is a novel component of the IFT system.

FAP133 is an IC associated with the retrograde IFT dynein motor

In *Chlamydomonas* a null mutation in the *DHC1b* gene results in very short, stumpy flagella that accumulate large amounts of IFT particles at their tips, suggesting that retrograde IFT requires this cytoplasmic dynein HC isoform (Pazour et al., 1999). In later studies, genetic and biochemical evidence indicated that D1bLIC is also an integral component of this retrograde IFT dynein (Hou et al., 2004; Perrone et al., 2003). However, in contrast to other dynein motor complexes that contain multiple HCs, no IC had yet been identified associated with this motor. Structural analysis of the 558-residue FAP133 polypeptide revealed a domain arrangement similar to that of other dynein ICs (Ogawa et al., 1995; Wilkerson et al., 1995), with six WD-repeats (and potentially a seventh at residues 295-391) in the C-terminal region. Furthermore, sequence alignment revealed that FAP133 is closely related to vertebrate WD34 (an uncharacterized protein and a possible ortholog of FAP133) and also to the IC of rat cytoplasmic dynein. On the basis of these findings, the proteomic analysis of *Chlamydomonas* flagella (Pazour et al., 2005), and the observation that FAP133 is involved in IFT, we predicted that FAP133 may associate with the retrograde IFT dynein motor.

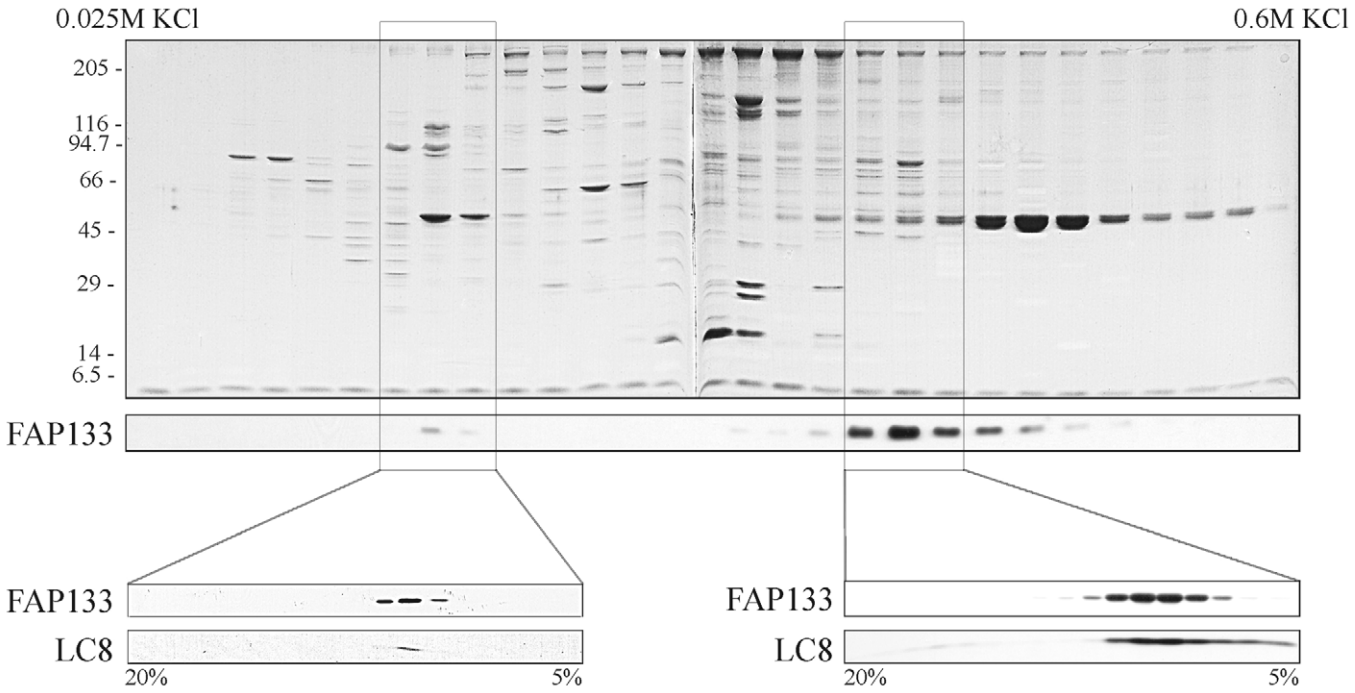

Fig. 8. FAP133 associates with LC8. Flagellar matrix components were fractionated using a Mono-Q anion-exchange column. The eluted fractions were separated in a 5-15% polyacrylamide gel and either stained with Coomassie Blue (upper panel) or transferred to a nitrocellulose membrane and probed for FAP133 (middle panel). The fractions that contained the two FAP133 peaks were pooled and further analyzed in two 5 ml 5-20% sucrose density gradients. Immunoblots of both gradients (lower left and right panel pairs) were probed for FAP133 and LC8. In both gradients FAP133 and LC8 were located in the same fractions at ~10 S.

Our finding that FAP133 does not localize at the peri-basal body region in the absence of DHC1b or D1bLIC provided strong genetic evidence to support this hypothesis.

IFT proteins present in flagella matrix extracts can be separated into at least four biochemically distinct complexes on sucrose-density gradients, including IFT complex A and complex B, the heterotrimeric kinesin-2 motor and the DHC1b-D1bLIC dynein complex (Cole et al., 1998; Perrone et al., 2003). Based on the requirement for IFT dynein to localize FAP133 at the basal body region, the behavior of ICs in other dynein complexes and consistent with our initial hypothesis, we expected FAP133 to co-migrate with DHC1b in a sucrose-density gradient. Instead, we found almost 90% of FAP133 migrating at ~10 S and only a small peak of this protein was detected in fractions containing the ~18 S form of DHC1b. Additional sedimentation experiments indicated that certain conditions, such as increased ionic-strength, non-ionic detergents and high hydrostatic pressure, induce the depletion of FAP133 from the ~18 S fractions owing to dissociation from the DHC1b-D1bLIC complex; some of these treatments also cause the further breakdown of the ~18 S IFT dynein motor into smaller subunits. Based on sedimentation analysis of both axonemal and cytoplasmic dyneins, the ~18 S form of the IFT dynein probably contains two HCs, whereas the ~12 S particle represents a HC monomer (for a review, see King, 2002). However, using a gel filtration column, we were able to purify DHC1b-D1bLIC-containing complexes that had a mass greater than that of the outer arm dynein. In these same fractions we also detected about 50% of the total FAP133 that was present in the flagella matrix extract. In addition, we also found that DHC1b co-immunoprecipitated with FAP133 from flagella matrix extracts. These results indicate that, whereas FAP133 is an integral part of the IFT dynein complex, the interaction between FAP133 and DHC1b-D1bLIC is relatively weak compared with other intra-dynein interactions, raising the possibility that it is subject to regulation in vivo.

FAP133, LC8 and the missing link to retrograde IFT

Chlamydomonas fla14 cells, which lack LC8, have very short flagella that accumulate IFT particles, indicating a defect in retrograde IFT (Pazour et al., 1998). Since LC8 is found in both cytoplasmic as well as outer arm and the I1/f inner arm axonemal dyneins, it may also associate directly with the retrograde IFT dynein motor. However, in previous studies LC8 did not co-purify with DHC1b or D1bLIC (Perrone et al., 2003) and it has been unclear why lack of LC8 results in defective retrograde IFT. Using various fractionation methods to separate flagella matrix components, we found that LC8 consistently co-purified with FAP133. Furthermore, immunoprecipitation using an antiserum against FAP133 pulled down a significant proportion of the LC8 that was present in the flagella matrix. These data indicate that LC8 interacts strongly with FAP133 and, therefore, may also be an integral component of the retrograde IFT dynein complex. Interestingly, analysis of the FAP133 sequence identified two potential degenerate LC8 binding sites in the region N-terminal of the WD repeats (see Fig. 1D), suggesting that these proteins interact directly as occurs in the major cytoplasmic dynein isoform. We propose that FAP133-LC8 represents an IC-LC complex that is readily dissociated from DHC1b-D1bLIC. It remains unclear whether this dynein sub-complex contains additional LC components as do the

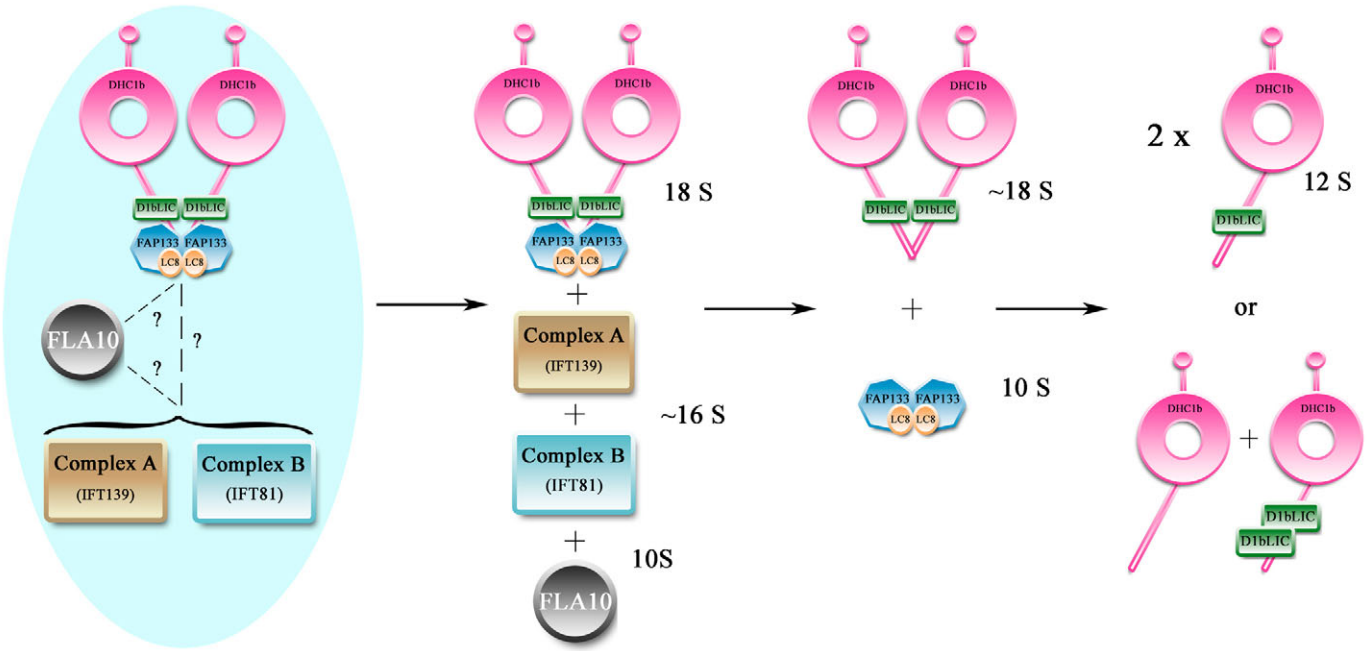

Fig. 9. Model of the retrograde IFT dynein motor. This model for associations involving the IFT dynein is based on the gel filtration, immunoprecipitation and sucrose-gradient data presented here. D1bLIC and an IC-LC complex, consisting of a FAP133 and an LC8 dimer, are predicted to associate independently with the N-terminal region of the DHC1b homodimer. The FAP133-LC8 subunit may mediate loading of the dynein motor complex onto an IFT particle scaffold that includes the FLA10 kinesin-2 subunit, complex A protein IFT139 and possibly complex B. Upon gel filtration, this dynein–kinesin-2–IFT complex assembly has a mass greater than that of the ~2 MDa outer dynein arm. Such IFT assemblies can dissociate into smaller complexes including intact dynein motors, IFT complex A, IFT complex B and heterotrimeric kinesin-2. The FAP133/LC8 subunit can further detach from the dynein complex and subsequently the DHC1b dimer may also dissociate to yield single HCs. It is currently unknown whether one D1bLIC remains bound to each DHC1b monomer or whether some HCs have two D1bLICs associated and others none.

analogous IC-LC structures in other dyneins (see King, 2002).

It has previously been shown that DHC1b and D1bLIC are normally located around the basal bodies of *fla14* cells but do not enter the flagella stubs, in contrast to the rest of the IFT proteins, which appear to accumulate at the tips (Pazour et al., 1998; Perrone et al., 2003). Similarly, we found that the majority of FAP133 was located primarily at the peri-basal body region in *fla14* cells but we did not detect any protein inside the flagella stubs. These observations suggest that DHC1b, D1bLIC and FAP133 associate within the cell body and are targeted to the basal bodies, even in the absence of LC8. However, LC8 appears to play a crucial role in the transition of the retrograde IFT dynein motor from the basal body region into the flagellum.

Architecture of the retrograde IFT dynein motor

Dynein ICs are known to play an essential role in maintaining the stability of the motor complex and in regulating the attachment of cargo. For example, the ICs that associate with cytoplasmic dynein serve as scaffolds that mediate interactions between the HCs, the three LC dimers as well as the p150 subunit of dynactin and other protein cargoes (Pfister et al., 2006; Vaughan and Vallee, 1995). Similarly, in *Chlamydomonas* axonemal outer arm dynein, both ICs (IC1 and IC2) associate with the HCs and LCs at the base of the motor complex and are required for the assembly and docking of the motor onto the A tubules of the outer doublets (King et al., 1991; Mitchell and Kang, 1991; Wilkerson et al., 1995). We found that the retrograde IFT dynein dissociates into two distinct sub-complexes; one that contains the HC and LIC and a second that contains FAP133 and LC8. Sedimentation of the FAP133-LC8 subunit at ~10 S in sucrose-density gradients indicates a particle of size similar to other IC-LC complexes. Thus FAP133 and LC8 both probably exist as dimers and potentially may associate with other components, such as Roadblock-LC7 and/or Tctex1 family LCs.

On the basis of our results and previously published data, we propose a model for the structural architecture of the retrograde IFT dynein motor (Fig. 9). We suggest that a FAP133-subunit dimer binds directly to the N-terminal region of DHC1b. LC8 might not be required for the association of FAP133 and DHC1b but is essential for the loading of the retrograde IFT dynein complex onto the anterograde transport system or onto other IFT cargoes, either by stabilizing the FAP133-LC8 sub-complex or by interacting directly with the IFT scaffold and/or IFT cargo components. In agreement with this model, we were able to purify by gel filtration particles that were larger than the ~2 MDa outer-arm dynein complex, and contained almost all flagellar DHC1b and D1bLIC, a portion of the soluble flagellar pool of IFT complex A IFT139 as well as at least 50% of the FAP133 and FLA10 kinesin-2. Although IFT81 from complex B was immunoprecipitated by the FAP133 antibody, only a very small amount of this protein

was present in the same gel-filtration fractions as dynein, FLA10 kinesin-2 and IFT139. The finding that a fraction of FAP133 always purified separately from DHC1b could indicate that the FAP133-LC8 sub-complex serves as an adaptor that readily dissociates from the DHC1b-D1bLIC complex when the motor needs to exchange cargoes. Alternatively, some fraction of FAP133 may be involved in a separate and currently unidentified process during IFT. It will be important to follow the movement of tagged FAP133 in vivo to determine whether or not FAP133 is indeed transported bi-directionally as predicted.

The model proposed here for the role of FAP133 in the retrograde IFT dynein motor predicts that retrograde IFT would be greatly compromised in the absence of FAP133. Indeed, in a recent study of conserved genes that are involved in flagellar activity in trypanosomes, it has been found that reduction of FAP133 protein levels by RNA interference resulted in cell clustering owing to flagellar dysfunction (Baron et al., 2007). The presence of FAP133 homologues in the genomes of vertebrates, sea urchins, insects and protists suggests a conserved function for this protein amongst ciliated organisms. However, the observation that a FAP133 homolog cannot be identified in *C. elegans*, which contains non-motile sensory cilia, raises the possibility that FAP133 functions only in motile cilia.

Materials and Methods

Strains and culture conditions

Wild-type *Chlamydomonas reinhardtii* (CC124), and the *fla10* (CC1919), *ida1* (CC2664), *ida4* (CC2670) *oda3* (CC2232), *oda5* (CC2236), *oda6* (CC2239), *pf14* (CC1032) and *pf18* (CC1036) mutant strains were obtained from the *Chlamydomonas* Center (Duke University, Durham NC). The *d1blic* (YH43), *dhc1b* (3088.4) and *fla14* (V64) mutant strains were provided by Gregory Pazour (University of Massachusetts Medical School, Worcester, MA). The *pf28pf30ssh1* strain (also referred to as WS4 isolate) was provided by Winfield Sale (Emory University School of Medicine, Atlanta, GA). Cells were grown in Tris-acetate-phosphate (TAP) (Gorman and Levine, 1965) or R medium at 22°C, aerated with 5% CO_2 and 95% air on a light-dark cycle (15 hours light 9 hours darkness).

Bioinformatics and molecular analysis of FAP133

Searches of the *Chlamydomonas* genomic and expressed sequence tag databases were performed using BLAST at http://genome.jgi-psf.org/Chlre3/Chlre3.home.html and http://est.kazusa.or.jp/en/plant/chlamy/EST/index.html, respectively. FAP133 homologues were identified using a TBLASTN search of the non-redundant database at NCBI (http://www.ncbi.nlm.nih.gov/BLAST/). Sequence alignment using CLUSTALW and generation of the neighbor-joining phylogenetic tree were performed at http://align.genome.jp. Domain analysis of FAP133 was achieved using SMART (http://dylan.embl-heidelberg.de/).

A cDNA (BP095745) encoding full-length FAP133 was obtained from the Kazusa DNA Research Institute. Northern and Southern blot analyses of *Chlamydomonas* RNA and genomic DNA samples, respectively, were performed using our standard methods (King and Patel-King, 1995).

Isolation and fractionation of flagella

Chlamydomonas flagella were isolated using the dibucaine method as described previously (King, 1995). Cells were grown in 2-8 l cultures and harvested by centrifugation. Purified flagella were resuspended in HME buffer (30 mM HEPES pH 7.4, 5 mM $MgSO_4$, 0.5 mM EGTA, 1 mM DTT) containing 25 mM potassium chloride (HMEK) or potassium acetate (HMEA) and supplemented with a protease inhibitor cocktail (Sigma, Catalog No. P9599). To study the effects of impaired anterograde IFT, wild-type and *fla10* cells were grown in TAP at 22°C in single 2-liter cultures. When the cultures reached log-phase, they were divided equally into two, one of which was transferred to a 32°C water-bath while the other was kept at 22°C; all cultures were placed under the same light conditions. After 1 hour, a small aliquot was removed from all cultures for immunofluorescence, whereas the rest of the cultures were used for isolating flagella as described above.

To obtain flagellar matrix proteins, purified flagella were resuspended in HMEK buffer, quick-frozen on dry ice and subsequently left to thaw at room temperature to facilitate disruption of the membrane. After three consecutive freeze-thaw cycles, flagella were pelleted by centrifugation at 10,000 rpm in a Hermle Z233 M-2 microfuge for 10 minutes and the supernatant removed and kept on ice until use. Alternatively, isolated flagella were demembranated with 1% Tergitol NP-40 (Sigma) or 0.1% Igepal CA-630 in HMEK buffer. Detergent-extracted axonemes were resuspended in HMEK buffer containing 10 mM ATP. After removing ATP-extracted components by centrifugation or following detergent extraction of whole flagella, axonemes were further treated with HME buffer containing 0.6 M NaCl to disrupt ionic interactions. Equivalent amounts of all fractions were loaded on 5-15% gradient SDS polyacrylamide gels and either stained with Coomassie Blue or blotted to nitrocellulose membrane for immunodetection.

Antibodies

For the production of antibody against FAP133, a 1.4 kb fragment of the *Chlamydomonas FAP133* cDNA (encoding residues 89-558) was amplified. The PCR product was inserted into the pMAL-c2 vector (New England Biolabs) across the *Xmn*I-*Xba*I restriction sites. This vector was used to transform *Escherichia coli* BL21 cells for the expression of a recombinant FAP133 polypeptide fused at the N-terminus with maltose-binding protein (MBP). The purified fusion protein was dialyzed against PBS pH 7.2 and was used as the immunogen to raise rabbit polyclonal antibody (CT248) (Covance, Denver, PA). The resulting antibody was affinity-purified against recombinant FAP133 after removing the MBP tag, essentially as described previously (Wakabayashi et al., 2007).

Other primary antibodies used in this study include: R4058 (vs LC8) (King and Patel-King, 1995), R5391 (vs LC2) (Patel-King et al., 1997), 1878A (vs IC1) (King et al., 1986) and anti-EB1 (Pedersen et al., 2003). Rabbit polyclonal antibodies against DHC1b and D1bLIC were generously provided by George Witman (University of Massachusetts Medical School, Worcester, MA). Mouse monoclonal antibodies against IFT81, IFT139 and IFT172 and a rabbit polyclonal antibody against FLA10 were generously provided by Douglas Cole (University of Idaho, Moscow, ID).

Protein fractionation

For sedimentation analysis, 200 μl of freshly prepared flagellar matrix extracts were layered onto 5 ml 5-20% sucrose-density gradients and centrifuged in a SW55Ti rotor for 10 hours at 30,000 rpm. Gel filtration was performed using a Superose-6 HR10/30 column (Amersham Biosciences), equilibrated with HMEK buffer supplemented with a protein inhibitor cocktail. Flagella from 8-liter cultures were extracted in the same buffer by freeze-thaw in a total volume of 5 ml. The flagellar matrix extract was then concentrated to 250 μl using an Amicon Ultra-4 filter unit and injected onto the column. The column was eluted with a 0.4 ml/minute flow rate and a total of 30 (0.75-ml) fractions were collected. Anion-exchange chromatography was performed on a Mono-Q HR5/5 column (Amersham Biosciences). Briefly, freshly prepared flagellar matrix extract was loaded onto the column that was previously equilibrated with HMEK buffer. The column was then washed with the same buffer for 10 minutes using a flow rate of 1 ml/minute. Elution was performed with a 0.5 ml/minute flow rate using a linear gradient of 0.025-0.6 M KCl with a total volume of 30 ml. Sixty fractions of 0.5 ml each were collected and analyzed. For subsequent sedimentation analysis, FAP133-containing fractions were pooled and concentrated using an Amicon Ultra-4 filter unit before layering onto a 5-20% sucrose-density gradient. Gel filtration and anion-exchange chromatography were performed using a Biologic II FPLC system (Bio-Rad).

Immunoprecipitations

For immunoprecipitation of FAP133, protein G-agarose beads (Pierce) were washed three times with TBS pH 7.2 supplemented with 3% BSA and then incubated with the anti-FAP133 antibody in the same buffer for 1 hour at 22°C. Beads were then washed three times with HMEK buffer and incubated with freshly prepared flagella matrix extract, for 1 hour at 22°C. The immunoprecipitated pellet was washed three times with HMEK buffer and finally resuspended in SDS gel sample buffer for further analysis. As a control, protein-G–agarose beads were treated only with 3% BSA before being added to the flagella matrix extract. Immunoprecipitation of IFT172 from flagellar extracts was performed similarly; immunoprecipitation with the IFT139 monoclonal antibody was as described previously (Pedersen et al., 2005).

SDS-PAGE and immunoblot analysis

Isolated *Chlamydomonas* flagella, flagellar fractions, and various protein samples were routinely solubilized in SDS gel sample buffer, separated by 5-15% gradient PAGE and stained with Coomassie Blue or blotted to nitrocellulose membranes for immunodetection using standard protocols.

Immunofluorescence microscopy

Chlamydomonas cells for immunofluorescence analysis were grown in TAP medium, harvested in mid-log phase by low-speed centrifugation at 90 ***g*** for 5 minutes and re-suspended in 10 mM Hepes pH 7.4. Microscope slides were treated before use with 1% poly-L-lysine (Sigma) in distilled water and air dried for 1 hour at 60°C. Cells in suspension were placed on treated slides and left to adhere for 5 minutes before fixing with methanol at –20°C for 10 minutes and air dried at room temperature for an additional 10 minutes. Subsequently, slides were placed in humidity chambers and re-hydrated with 1% Igepal CA-630 (Sigma) in PBS pH 7.2

for 10 min. After briefly rinsing with PBS, cells were treated for 1 hour at room temperature with blocking buffer containing 3% normal goat serum, 1% BSA, 1% cold-water-fish gelatin, 0.1% Igepal CA-630 and 0.05% Tween-20 in PBS. All antibodies used for immunofluorescence microscopy were diluted in PBS buffer containing 1% BSA, 0.1% cold-water-fish gelatin and 0.05% Tween-20. Cells were incubated with primary antibodies for 1-2 hours at 22°C or alternatively for 16 hours at 4°C, washed four times for 5 minutes with PBS and incubated with either Alexa Fluor 488-conjugated anti-mouse or Alexa Fluor 568-conjugated anti-rabbit secondary antibodies (Invitrogen) for 1 hour. Slides were washed four times for 5 minutes with PBS, dehydrated in a series of 30, 70 and 100% ethanol baths, air dried and mounted with coverslips using a glycerol-based mounting medium containing DABCO (Sigma) as an anti-fade agent. Stained cells were viewed on an Olympus BX51 epifluorescence microscope (Olympus America Inc.), equipped with PlanApo 60×/1,4 and 100×/1,35 oil immersion lenses, and images were acquired with a Magnafire cool-CCD digital camera (Optronics).

We thank Oksana Gorbatyuk (University of Connecticut Health Center, Farmington, CT) for assistance with preliminary biochemical analysis of FAP133, Gregory Pazour and Winfield Sale for *Chlamydomonas* mutant strains, and Douglas Cole and George Witman for generously providing antibodies and for helpful discussions. This work was supported by grant GM51293 from the National Institutes of Health and an investigator award from the Patrick and Catherine Donaghue Medical Research Foundation to S.M.K., and by grants from the Danish Natural Science Research Council (no. 272-05-0411) and the Novo Nordisk Foundation to L.B.P.

References

Baron, D., Ralston, K., Kabututu, Z. and Hill, K. (2007). Functional genomics in *Trypanosoma brucei* identifies evolutionarily conserved components of motile flagella. *J. Cell Sci.* **120**, 478-491.

Christensen, S., Pedersen, L., Schneider, L. and Satir, P. (2007). Sensory cilia and integration of signal transduction in human health and disease. *Traffic* **8**, 97-109.

Cole, D. G. (2003). The intraflagellar transport machinery of *Chlamydomonas reinhardtii*. *Traffic* **4**, 435-442.

Cole, D., Chinn, S., Wedaman, K., Hall, K., Vuong, T. and Scholey, J. (1993). A novel heterotrimeric kinesin purified from sea urchin eggs. *Nature* **366**, 268-270.

Cole, D. G., Diener, D. R., Himelblau, A. L., Beech, P. L., Fuster, J. C. and Rosenbaum, J. L. (1998). *Chlamydomonas* kinesin-II-dependent intraflagellar transport (IFT): IFT particles contain proteins required for ciliary assembly in *Caenorhabditis elegans* sensory neurons. *J. Cell Biol.* **141**, 993-1008.

DiBella, L. M. and King, S. M. (2001). Dynein motors of the *Chlamydomonas* flagellum. *Int. Rev. Cytol.* **210**, 227-268.

Follit, J., Tuft, R., Fogarty, K. and Pazour, G. J. (2006). The intraflagellar transport protein IFT20 is associated with the Golgi complex and is required for cilia assembly. *Mol. Biol. Cell* **17**, 3781-3792.

Gorman, D. and Levine, R. (1965). Cytochrome f and plastocyanin: their sequence in the photosynthetic electron transport chain of *Chlamydomonas reinhardtii*. *Proc. Natl. Acad. Sci. USA* **54**, 1665-1669.

Grissom, P. M., Vaisberg, E. A. and McIntosh, J. R. (2002). Identification of a novel light intermediate chain (D2LIC) for mammalian cytoplasmic dynein 2. *Mol. Biol. Cell* **13**, 817-829.

Henson, J. H., Cole, D. G., Roesener, C. D., Capuano, S., Mendola, R. J. and Scholey, J. M. (1997). The heterotrimeric motor protein kinesin-II localizes to the midpiece and flagellum of sea urchin and sand dollar sperm. *Cell Motil. Cytoskeleton* **38**, 29-37.

Hou, Y., Pazour, G. J. and Witman, G. B. (2004). A dynein light intermediate chain, D1bLIC, is required for retrograde intraflagellar transport. *Mol. Biol. Cell* **15**, 4382-4394.

Hou, Y., Qin, H., Follit, J. A., Pazour, G. J., Rosenbaum, J. L. and Witman, G. B. (2007). Functional analysis of an individual IFT protein: IFT46 is required for transport of outer dynein arms into flagella. *J. Cell Biol.* **176**, 653-665.

Huang, B., Rifkin, M., Luck, D. and Kozler, V. (1977). Temperature-sensitive mutations affecting flagellar assembly and function in *Chlamydomonas reinhardtii*. *J. Cell Biol.* **72**, 67-85.

Iomini, C., Babaev-Khaimov, V., Sassaroli, M. and Piperno, G. (2001). Protein particles in *Chlamydomonas* flagella undergo a transport cycle consisting of four phases. *J. Cell Biol.* **153**, 13-24.

Johnson, K. A. and Rosenbaum, J. L. (1992). Polarity of flagellar assembly in *Chlamydomonas*. *J. Cell Biol.* **119**, 1605-1611.

King, S. M. (1995). Large-scale isolation of *Chlamydomonas* flagella. *Methods Cell Biol.* **47**, 9-12.

King, S. M. (2002). Dynein motors: structure, mechanochemistry and regulation. In *Molecular Motors* (ed. M. Schliwa), pp. 45-78. Weinheim: Wiley.

King, S. M. and Patel-King, R. S. (1995). The $M_{(r)}$=8,000 and 11,000 outer arm dynein light chains from *Chlamydomonas* flagella have cytoplasmic homologues. *J. Biol. Chem.* **270**, 11445-11452.

King, S. M., Otter, T. and Witman, G. B. (1986). Purification and characterization of *Chlamydomonas* flagellar dyneins. *Meth. Enzymol.* **134**, 291-306.

King, S. M., Wilkerson, C. G. and Witman, G. B. (1991). The M_r 78,000 intermediate chain of *Chlamydomonas* outer arm dynein interacts with α-tubulin *in situ*. *J. Biol. Chem.* **266**, 8401-8407.

Kozminski, K. G., Johnson, K. A., Forscher, P. and Rosenbaum, J. L. (1993). A motility in the eukaryotic flagellum unrelated to flagellar beating. *Proc. Natl. Acad. Sci. USA* **90**, 5519-5523.

Kozminski, K., Beech, P. and Rosenbaum, J. L. (1995). The *Chlamydomonas* kinesin-like protein FLA10 is involved in motility associated with the flagellar membrane. *J. Cell Biol.* **131**, 1517-1527.

Lo, K. W.-H., Naisbitt, S., Fan, J.-S., Sheng, M. and Zhang, M. (2001). The 8 kDa dynein light chain binds to its targets via a conserved "K/R-X-T-Q-T" motif. *J. Biol. Chem.* **276**, 14059-14066.

Marshall, W. F. and Rosenbaum, J. L. (2001). Intraflagellar transport balances continuous turnover of outer doublet microtubules: implications for flagellar length control. *J. Cell Biol.* **155**, 405-414.

Mikami, A., Tynan, S., Hama, T., Luby-Phelps, K., Saito, T., Crandall, J., Besharse, J. and Vallee, R. B. (2002). Molecular structure of cytoplasmic dynein 2 and its distribution in neuronal and ciliated cells. *J. Cell Sci.* **115**, 4801-4808.

Mitchell, D. R. and Kang, Y. (1991). Identification of *oda6* as a *Chlamydomonas* dynein mutant by rescue with the wild-type gene. *J. Cell Biol.* **113**, 835-842.

Ogawa, K., Kamiya, R., Wilkerson, C. G. and Witman, G. B. (1995). Interspecies conservation of outer arm dynein intermediate chain sequences defines two intermediate chain subclasses. *Mol. Biol. Cell* **6**, 685-696.

Pan, J., Wang, Q. and Snell, W. (2005). Cilium-generated signaling and cilia-related disorders. *Lab. Invest.* **85**, 452-463.

Pan, X., Ou, G., Civelekoglu-Scholey, G., Blacque, O. E., Endres, N. F., Tao, L. M., Mogilner, A., Leroux, M. R., Vale, R. D. and Scholey, J. M. (2006). Mechanism of transport of IFT particles in *C. elegans* cilia by the concerted action of kinesin-II and OSM-3 motors. *J. Cell Biol.* **174**, 1035-1045.

Patel-King, R. S., Benashski, S. E., Harrison, A. and King, S. M. (1997). A *Chlamydomonas* homologue of the putative murine *t* complex distorter Tctex-2 is an outer arm dynein light chain. *J. Cell Biol.* **137**, 1081-1090.

Pazour, G. J., Wilkerson, C. G. and Witman, G. B. (1998). A dynein light chain is essential for the retrograde particle movement of intraflagellar transport (IFT). *J. Cell Biol.* **141**, 979-992.

Pazour, G. J., Dickert, B. L. and Witman, G. B. (1999). The DHC1b (DHC2) isoform of cytoplasmic dynein is required for flagellar assembly. *J. Cell Biol.* **144**, 473-481.

Pazour, G., Agrin, N., Leszyk, J. and Witman, G. (2005). Proteomic analysis of a eukaryotic flagellum. *J. Cell Biol.* **170**, 103-113.

Pedersen, L., Miller, M., Geimer, S., Leitch, J., Rosenbaum, J. L. and Cole, D. (2005). *Chlamydomonas* IFT172 is encoded by *FLA11*, interacts with CrEB1, and regulates IFT at the flagellar tip. *Curr. Biol.* **15**, 262-266.

Pedersen, L. B., Geimer, S. and Rosenbaum, J. L. (2006). Dissecting the molecular mechanisms of intraflagellar transport in *Chlamydomonas*. *Curr. Biol.* **16**, 450-459.

Pedersen, L. B., Geimer, S., Sloboda, R. D. and Rosenbaum, J. L. (2003). The microtubule plus end-tracking protein EB1 is localized to the flagellar tip and basal bodies in *Chlamydomonas reinhardtii*. *Curr. Biol.* **13**, 1969-1974.

Perrone, C., Tritschler, D., Taulman, P., Bower, R., Yoder, B. and Porter, M. (2003). A novel dynein light intermediate chain colocalizes with the retrograde motor for intraflagellar transport at sites of axoneme assembly in *Chlamydomonas* and mammalian cells. *Mol. Biol. Cell* **14**, 2041-2056.

Pfister, K. K., Shah, P. R., Hummerich, H., Russ, A., Cotton, J., Annuar, A. A., King, S. M. and Fisher, E. M. C. (2006). Genetic analysis of the cytoplasmic dynein subunit families. *PLoS Genet.* **2**, e1.

Piperno, G. and Mead, K. (1997). Transport of a novel complex in the cytoplasmic matrix of *Chlamydomonas* flagella. *Proc. Natl. Acad. Sci. USA* **94**, 4457-4462.

Porter, M. E., Bower, R., Knott, J. A., Byrd, P. and Dentler, W. (1999). Cytoplasmic dynein heavy chain 1b is required for flagellar assembly in *Chlamydomonas*. *Mol. Biol. Cell* **10**, 693-712.

Qin, H., Diener, D. R., Geimer, S., Cole, D. G. and Rosenbaum, J. L. (2004). Intraflagellar transport (IFT) cargo: IFT transports flagellar precursors to the tip and turnover products to the cell body. *J. Cell Biol.* **164**, 255-266.

Qin, H., Wang, Z., Diener, D. R. and Rosenbaum, J. L. (2007). Intraflagellar transport protein 27 is a small G protein involved in cell-cycle control. *Curr. Biol.* **17**, 193-202.

Rosenbaum, J. L. and Witman, G. B. (2002). Intraflagellar transport. *Nat. Rev. Mol. Cell Biol.* **3**, 813-825.

Schafer, J., Haycraft, C., Thomas, J., Yoder, B. and Swoboda, P. (2003). XBX-1 encodes a dynein light intermediate chain required for retrograde intraflagellar transport and cilia assembly in *Caenorhabditis elegans*. *Mol. Biol. Cell* **14**, 2057-2070.

Scholey, J. M. (2003). Intraflagellar transport. *Annu. Rev. Cell Dev. Biol.* **19**, 423-443.

Signor, D., Wedaman, K. P., Orozco, J. T., Dwyer, N. D., Bargmann, C. I., Rose, L. S. and Scholey, J. M. (1999). Role of a class DHC1b dynein in retrograde transport of IFT motors and IFT raft particles along cilia, but not dendrites, in chemosensory neurons of living *Caenorhabditis elegans*. *J. Cell Biol.* **147**, 519-530.

Snow, J. J., Ou, G., Gunnarson, A. L., Walker, M. R. S., Zhou, H. M., Brust-Mascher, I. and Scholey, J. M. (2004). Two anterograde intraflagellar transport motors cooperate to build sensory cilia on *C. elegans* neurons. *Nature Cell Biol.* **6**, 1109-1113.

Stolc, V., Samanta, M., Tongprasit, W. and Marshall, W. (2005). Genome-wide transcriptional analysis of flagellar regeneration in *Chlamydomonas reinhardtii* identifies orthologs of ciliary disease genes. *Proc. Natl. Acad. Sci. USA* **102**, 3703-3707.

Vallee, R. B., Williams, J., Varma, D. and Barnhart, L. (2004). Dynein: an ancient motor protein involved in multiple modes of transport. *J. Neurobiol.* **58**, 189-200.

Vaughan, K. T. and Vallee, R. B. (1995). Cytoplasmic dynein binds dynactin through a direct interaction between the intermediate chains and p150Glued. *J. Cell Biol.* **131**, 1507-1516.

Wakabayashi, K., Sakato, M. and King, S. M. (2007). Protein modification to probe intradynein interactions and *in vivo* redox state. *Methods Mol. Biol.* **392**, 71-83.

Walther, Z., Vashishtha, M. and Hall, J. L. (1994). The *Chlamydomonas FLA10* gene encodes a novel kinesin-homologous protein. *J. Cell Biol.* **126**, 175-188.

Wilkerson, C. G., King, S. M., Koutoulis, A., Pazour, G. J. and Witman, G. B. (1995). The 78,000 $M_{(r)}$ intermediate chain of *Chlamydomonas* outer arm dynein is a WD-repeat protein required for arm assembly. *J. Cell Biol.* **129**, 169-178.

Witman, G. B. (1975). The site of *in vivo* assembly of flagellar microtubules. *Ann. N. Y. Acad. Sci.* **253**, 178-191.

Yamazaki, H., Nakata, T., Okada, Y. and Hirokawa, N. (1995). KIF3A/B: a heterodimeric kinesin superfamily protein that works as a microtubule plus end-directed motor for membrane organelle transport. *J. Cell Biol.* **130**, 1387-1399.